EIS at carbon fiber cylindrical microelectrodes

Leatham Landon-Lane, Aaron T. Marshall, David A. Harrington

December 2019

Electrochemistry Communications 109 (2019) 106566

Contents lists available at ScienceDirect

Electrochemistry Communications

journal homepage: www.elsevier.com/locate/elecom

EIS at carbon fiber cylindrical microelectrodes

Leatham Landon-Lane[a], Aaron T. Marshall[a,*], David A. Harrington[b,*]

[a] Department of Chemical and Process Engineering, University of Canterbury, Christchurch 8140, New Zealand
[b] Department of Chemistry, University of Victoria, Victoria, BC, V8W 2Y2, Canada

ARTICLE INFO

Keywords:
Mass transport impedance
Cylindrical diffusion
Carbon fiber
Microelectrode
EIS

ABSTRACT

The theoretical mass-transport impedance at cylindrical microelectrodes has been known for some time, but an experimental verification is given here for the first time, using carbon fiber electrodes taken from a commercial carbon felt. Nonlinear least-squares fitting of the impedance spectrum of a redox couple at the reversible potential enables accurate evaluation of a composite parameter containing the standard rate constant and mean diffusivity, without measuring the fiber diameter, length or area.

1. Introduction

The use of fiber-based materials in electrochemistry has seen a resurgence recently, with the use of carbon felts as electrodes in redox flow batteries and electrospun polymers in emerging energy technologies. It is important to be able to characterize individual fibers and relate this information to the properties of the assembled material. At the time when microelectrodes were being developed, there was an interest in cylindrical microelectrodes [1–6], but they were harder to manipulate and there were indications that convection effects disrupted the desired radial diffusion [7,8]. There are reports of fits of cyclic voltammetry and chronoamperometry data to numerical simulations involving cylindrical diffusion [2]. The mass transport impedance has an analytical solution, but has apparently not been applied to the case of long cylindrical microelectrodes, for which the radius is less than the diffusion length. We here study the $Fe(CN)_6^{3-}/Fe(CN)_6^{4-}$ redox couple at individual carbon fibers, and show that electrochemical impedance spectroscopy (EIS) enables accurate extraction of the standard rate constant.

The dc diffusion field between two concentric cylinders has a logarithmic dependence on the cylinder radii, Eq. (1), as known for a long time, e.g., from the analogous current distribution problem [9].

$$c(r_\delta) - c(r_0) = -\frac{rJ(r)}{D}\ln\frac{r_\delta}{r_0} \tag{1}$$

Here r_δ and r_0 are the radii of the outer and inner cylinders, D is the diffusivity, $J(r)$ is the radial flux (mol m^{-2} s^{-1}), and the product $rJ(r)$ is independent of r. The case of interest here is a large solution volume, $r_\delta \to \infty$. In that case, the logarithmic factor tends to infinity and so the system does not reach a true steady state. However, as in the 1-D semi-infinite case, we proceed to solve the ac problem as though there were a steady state, recognizing that the impedance will go to infinity at low frequencies.

Fleischmann et al. [8] derived the impedance for a quasireversible redox couple at a cylindrical microelectrode. The solution was given as a complicated expression involving the Kelvin functions Kei and Ker. They stated that the real and imaginary parts increase to infinity because there is no steady state, but their complex-plane plot suggests that the imaginary part tends to a constant value at low frequencies. Later, Jacobsen and West [10] gave the solution for the dimensionless mass transport impedance in terms of Bessel functions as Eq. (2), where K_0 and K_1 are the modified Bessel functions of the second kind of order 0 and 1, and τ_d is a diffusion time constant.

$$z = \frac{\tilde{c}D}{\tilde{J}r_0} = \frac{K_0(\sqrt{i\omega\tau_d})}{\sqrt{i\omega\tau_d}K_1(\sqrt{i\omega\tau_d})} \tag{2}$$

$$\tau_d = r_0^2/D \tag{3}$$

They correctly pointed out that the imaginary part tends to a constant value of $-\pi/4$ at zero frequency. (The similar case of insertion and diffusion into a cylindrical electrode was earlier solved in terms of Bessel functions by Barral et al. [11]).

The mass transport impedance in usual units is given by $Z_d = \sigma'\sqrt{\tau_d}z$, which replaces $Z_d = \sigma'/\sqrt{i\omega}$ for the more usual 1-D semi-infinite case. Aside from this substitution, the mass transport impedance is coupled to the reaction kinetics in the usual way. For the standard redox reaction and kinetics, Eqs. (4,5)

* Corresponding authors.
E-mail addresses: leatham.landon-lane@pg.canterbury.ac.nz (L. Landon-Lane), aaron.marshall@canterbury.ac.nz (A.T. Marshall), dharr@uvic.ca (D.A. Harrington).

https://doi.org/10.1016/j.elecom.2019.106566
Received 11 September 2019; Received in revised form 12 October 2019; Accepted 14 October 2019
Available online 31 October 2019

$$R \rightleftarrows P + e^- \quad (4)$$

$$j/F = k_f c_R - k_b c_P \quad (5)$$

the derivation of the Randles circuit [12,13] gives σ' as in Eq. (6).

$$\sigma' = \sqrt{2}\sigma = R_{ct}(k_f D_R^{-1/2} + k_b D_P^{-1/2}) \quad (6)$$

In coupling the mass transport, and for the rest of the paper, we make the common assumption that $D_R = D_P = D$, and σ' then reduces to Eq. (7), where $k = k_f + k_b$. It is convenient to fit directly to the composite parameter ψ, Eq. (8), which is independent of electrode area.

$$\sigma' = R_{ct} k D^{-1/2} \quad (7)$$

$$\psi = \sigma'/R_{ct} = k/\sqrt{D} \quad (8)$$

If both species are present in equal concentrations c^b and their activity coefficients are equal, then at the reversible potential the standard rate constant $k^o = k_f = k_b$, and the simple relationships of Eqs. (9)–(11) apply.

$$\psi = 2k^o/\sqrt{D} \quad (9)$$

$$R_{ct} = RT/F^2 c^b k^o \quad (10)$$

$$\sigma' = 2RT/F^2 c^b D^{1/2} \quad (11)$$

2. Materials and methods

Single carbon fibers were extracted from a carbon felt sample (GFE-1, Ceramaterials, USA) and glued to electrical wire using carbon glue. The wire was housed in a glass capillary tube and the end sealed with epoxy resin, leaving only the carbon fiber exposed to the electrolyte. Data were collected at 23 ± 1 °C.

SEM images of the felt showed fiber diameters averaging 10 μm with a standard deviation of 1 μm.

Detailed EIS data were collected for two fibres, but the results are here reported for a single 3.4 mm long fibre, which had lower EIS noise.

The solution was 1 mol dm^{-3} KNO_3 with 10.0 mmol dm^{-3} each of $K_3Fe(CN)_6$ (Vickers Laboratories Ltd) and $K_4Fe(CN)_6$ (BDH AnalaR). The diffusivities in 1 mol dm^{-3} KNO_3 were calculated from the limiting current reached during steady state polarisation curves on a polished gold rotating disk electrode (5 mm diameter, Pine Research Instrumentation), rotated at speeds from 100 to 600 rpm. The Levich equation was applied to relate the limiting current to the diffusivities, which were found to be 8.6×10^{-6} cm^2 s^{-1} for $Fe(CN)_6^{4-}$ and 8.37×10^{-6} cm^2 s^{-1} for $Fe(CN)_6^{3-}$. Here we use the mean value $8.50 \pm 0.05 \times 10^{-6}$ cm^2 s^{-1}, where the quoted 1σ error is somewhat arbitrarily estimated so that $\pm 2\sigma$ spans the two measured diffusivities. This is similar to the literature mean value in 0.5 mol dm^{-3} K_2SO_4 of 8.45×10^{-6} cm^2 s^{-1} [14].

Potentiostatic EIS data were collected with a Gamry 3000 potentiostat, and were fitted to the impedance expression (12) for the Randles circuit for cylindrical diffusion and with a CPE replacing the double-layer capacitance.

$$Z = R_u + 1/(Y_0(i\omega)^\phi + 1/(R_{ct}(1 + \psi\sqrt{\tau_d}z))) \quad (12)$$

The complex nonlinear least squares fitting was done using Maple's NLPSolve routine using the nonlinearsimplex option [15], with a custom calling program [16] that also derives the standard errors in the usual way, i.e., from the values of the derivatives of the impedance with respect to the parameters at the minimum [17]. No weighting was used. Fitting failed to converge using the Bessel function expression (2), probably because the numerical evaluation of the real and imaginary parts is subject to error. Therefore the expression was replaced by the approximation

$$z = \ln\left(\frac{1 + \sqrt{i\omega\tau_d}}{\sqrt{i\omega\tau_d}}\right) \quad (13)$$

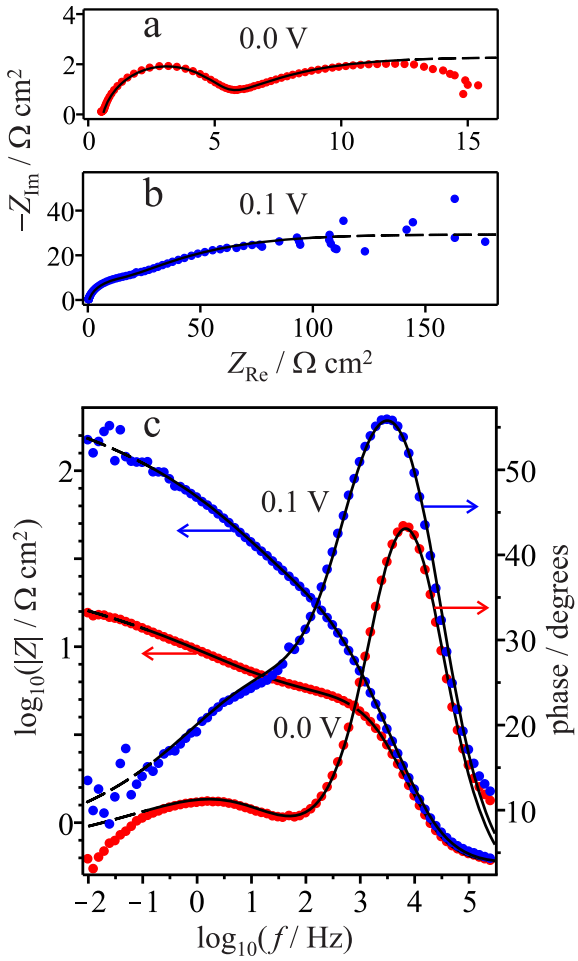

Fig. 1. Impedance spectra for a carbon fiber. Red points are experimental data at the reversible potential, blue points are at an overpotential of + 0.1 V. Black solid lines are fitted curves; dashed lines are extensions into the lower frequency region that was not used in the fit. (For interpretation of the references to colour in this figure legend, the reader is referred to the web version of this article.)

for which the real and imaginary parts have analytical expressions known to Maple. It matches the logarithmic dependence on frequency of the real part and constant imaginary part $-\pi/4$ at low frequencies and $(i\omega)^{-1/2}$ dependence at high frequencies [10] and interpolates between them. The relative errors (with respect to Eq. (2)) in the real and imaginary parts do not exceed 4%. For the fitted data, the resulting systematic error in the parameters can be estimated by individually varying the parameters to find the minimum in the residual sum of squares. For example, for the 0 V case below, these errors were about 2% for ψ, 9% for τ_d and 1% for R_{ct}. The statistical errors given below used the fitted function, but in the plots comparing the experimental and theoretical values, the full Eq. (2) is shown.

The data were analyzed without regard to the electrode area, but Fig. 1 presents data relative to the area, which was estimated from the length and the radius determined from τ_d as described below.

3. Results and discussion

Fig. 1 shows impedance spectra at two selected potentials. As usual, the high-frequency semicircle in the Nyquist plots arises from the charge-transfer resistance and double-layer capacitance. The lower-frequency feature is the mass transport impedance, which rises to a plateau as predicted. In the case of the reversible potential, at the lowest measured frequencies the imaginary part of the impedance

decreased again, possibly due to convection. At higher overpotentials, the low-frequency region became noisy and this decrease was not seen. The value of τ_d determines the frequency at which the rise to the plateau occurs and the value of σ' determines the height of the plateau.

At the reversible potential, the fitted parameters were $\psi = 5.28 \pm 0.07\,s^{-1/2}$, $\tau_d = 13.7 \pm 0.4$ ms, $R_{ct} = 6470 \pm 30\,\Omega$, $Y_0 = 56 \pm 2\,nF\,s^{1-\phi}$, $\phi = 0.843 \pm 0.003$ and $R_u = 790 \pm 9\,\Omega$. Using Eq. (3), the radius of the fiber was estimated from the values of τ_d and the mean diffusivity (Section 2) to be 3.42 ± 0.05 μm.

The standard rate constant calculated from Eq. (9) is $k^o = 7.70 \pm 0.11 \times 10^{-3}$ cm s^{-1}. The value of R_{ct} at the reversible potential can then be estimated from Eq. (10) to be 3.4 Ω cm^2. The errors in k^o and r_0 are dominated by the fitting errors in ψ and τ_d respectively, and not the error in the mean diffusivity. The quoted errors are fitting errors only, and a more extensive study of many fibers will be required to clarify systematic errors. As in impedance methods for other geometries, no measurement of the surface area of the fiber is required.

If the measured area is available, then a consistency check may be carried out by comparing R_{ct} above with the directly fitted R_{ct} in Ohms multiplied by the area. In the present case, the area was estimated from the radius found above and the known length, which gives $R_{ct} = 4.7\,\Omega$ cm^2. Instead of starting with a known mean diffusivity, an alternative approach to this analysis would be to use the measured radius to estimate the diffusivity, and in turn the rate constant.

Literature standard rate constants for the $Fe(CN)_6^{3-/4-}$ system vary widely depending on the solution, the type of carbon surface and the surface pretreatment, and span the range $0.005 - 0.5$ cm s^{-1} [18]. For the fastest rate constants ($\gtrsim 0.1$ cm s^{-1}) an activation procedure is generally required [19]. Lower values similar to that obtained here are typically obtained for unactivated surfaces such as regularly polished glassy carbon 0.005 cm s^{-1} [20,18] or carbon paste $0.001 - 0.007$ cm s^{-1} [21].

The analysis here assumes smooth surfaces, or at least a roughness scale small compared to the radius, in which case the true rate constant is the quoted value divided by the roughness factor, and the radius determined will be an average value. The effective double-layer capacitance calculated from the Brug formula (Eq. (8.12), Ref. [12]) is small, 12 μF cm^{-2}, similar to literature values [2,22] for untreated fibers. Much higher capacitances are found for activated and severely roughened surfaces, for which the effective radius may underestimate the true radius [2].

A distribution of rate constants is expected for the different fibers in a carbon felt [24–26], and the present method can be useful in determining the variation in rate constants. For the type of fibers used here, numerical modeling of voltammograms gave standard rate constants for 13 fibers with a mean of 7.3×10^{-3} cm s^{-1} and a standard deviation of 4.7×10^{-3} cm s^{-1}. The individual determinations by the impedance method were more accurate.

Measurements were also carried out away from the reversible potential. These could also be fitted to the same impedance expression, but the high-frequency semicircle and the mass-transport feature were less well resolved, which led to higher errors in τ_d and the other parameters. Allowing for the larger errors, the parameters τ_d, Y_0, ϕ and R_s did not depend much on potential as expected. The parameters R_{ct} and ψ are expected to be potential dependent, and although they were higher for higher overpotentials, the potential dependence was weak.

Simulations showed that the potential dependence did not fit the expectations of a simple one-electron reaction with Tafel-like potential dependence of rate constants. Non-ideal behavior for the $Fe(CN)_6^{3-/4-}$ system at C electrodes has been seen before and attributed to adsorption [27] or other interactions with the surface [19]. In the specific case of KNO_3 solutions, Fletcher and Varley saw Tafel slopes as low as 62 mV/decade and invoked a chemical step [23]. Another possibility is electrode aging due to deposition of a film, which limits electron transfer and reduces the potential dependence, though the constancy of the double-layer parameters argues against this mechanism. We also note that measurements away from the reversible potential can be affected by ohmic drop along the fiber itself, which has a resistance of the order of 400 Ω mm^{-1}.

Another possibility is that convection, which dogged early experiments with microcylindrical electrodes, is operating at higher overpotentials, where a dc concentration gradient is present in solution. Unlike other methods, EIS can fully determine the standard rate constant without significant excursions away from the reversible potential. There is therefore no requirement for a dc concentration gradient, only an ac one, for which modern instruments excel at noise rejection. The resolution of this issue is outside the scope of the present work, where good results were always achieved for pristine fibers at the reversible potential.

4. Conclusions

The Bessel function form for the impedance of the cylindrical diffusion problem was experimentally verified for the first time by nonlinear least-squares fitting to impedance data measured for the $Fe(CN)_6^{3-/4-}$ redox system at carbon fiber electrodes. Accurate results were facilitated by fitting directly to an approximation of the theoretical expression for the impedance. By making the combined parameter $k/\sqrt{D}$ one of the fit parameters, the need for error propagation was minimized and the rate constant could be accurately found. Provided the mean diffusivity is known, this method does not require measurements of the electrode length, radius or area.

Acknowledgements

Financial support is acknowledged from the Natural Sciences and Engineering Council of Canada (Discovery Grant RGPIN-2017-04045) and the University of Canterbury (PhD scholarship for L. Landon-Lane).

References

[1] S.A. Schuette, R.L. McCreery, Anal. Chem. 58 (1986) 1778–1782.
[2] P.M. Kovach, M.R. Deakin, R.M. Wightman, J. Phys. Chem. 90 (1986) 4612–4617.
[3] J. Wang, P. Tuzhi, V. Villa, J. Electroanal. Chem. 234 (1987) 119–131.
[4] K. Aoki, H. Kaneko, J. Electroanal. Chem. 247 (1988) 17–27.
[5] K.B. Oldham, J. Electroanal. Chem. 313 (1991) 3–16.
[6] A. Neudeck, J. Dittrich, J. Electroanal. Chem. 313 (1991) 37–59.
[7] H.P. Wu, R.L. McCreery, Anal. Chem. 61 (1989) 2347–2352.
[8] M. Fleischmann, S. Pons, J. Daschbach, J. Electroanal. Chem. 317 (1991) 1–26.
[9] C. Kasper, Trans. Electrochem. Soc. 77 (1940) 353–363.
[10] T. Jacobsen, K. West, Electrochim. Acta 40 (1995) 255–262.
[11] G. Barral, J.P. Diard, C. Montella, Electrochim. Acta 29 (1984) 239–246.
[12] A. Lasia, Electrochemical Impedance Spectroscopy and its Applications, Springer, NY, 2014.
[13] R. de Levie, L. Pospíšil, J. Electroanal. Chem. 22 (1969) 277–290.
[14] D.H. Angell, T. Dickinson, J. Electroanal. Chem. 35 (1972) 55–72.
[15] Maple version 2017, Maplesoft, a division of Waterloo Maple Inc., Waterloo, Ontario,http://www.maplesoft.com.
[16] Program immfit, available at the Maple Applications Center,http://www.maplesoft.com/applications/view.aspx?SID=154540.
[17] D.M. Bates, D.G. Watts, Nonlinear Regression Analysis and its Applications, Wiley, 1988, p. 53.
[18] R.L. McCreery, Chem. Rev. 108 (2008) 2646–2687.
[19] P. Chen, R.L. McCreery, Anal. Chem. 68 (1996) 3958–3965.
[20] W.J. Blaedel, R.C. Engstrom, Anal. Chem. 50 (1978) 476–479.
[21] Z. Galus, R.N. Adams, J. Phys. Chem. 67 (1963) 866–871.
[22] M.A. Miller, A. Bourke, N. Quill, J.S. Wainright, R.P. Lynch, D.N. Buckley, R.F. Savinell, J. Electrochem. Soc. 163 (2016) A2095–A2102.
[23] S. Fletcher, T.S. Varley, Phys. Chem. Chem. Phys. 13 (2011) 5359–5364.
[24] T.J. Rabbow, M. Trampert, P. Pokorny, P. Binder, A.H. Whitehead, Electrochimica 173 (2015) 24–30.
[25] M.L. Perry, A.Z. Weber, J. Electrochem. Soc. 163 (2016) A5064–A5067.
[26] T. Tichter, D. Andrae, J. Mayer, J. Schneider, M. Gebhard, C. Roth, Phys. Chem. Chem. Phys. 21 (2019) 9061–9068.
[27] R. Sohr, L. Müller, R. Landsberg, J. Electroanal. Chem. 50 (1974) 55–63.